

Highly efficient synthesis of Fe-containing mesoporous materials by using semi-fluorinated surfactant and their high activities in Friedel–Crafts alkylations

Yunchen Du, Sen Liu, Yanyan Ji, Yonglai Zhang,
Fujian Liu, Qian Gao, Feng-Shou Xiao*

*State Key Laboratory of Inorganic Synthesis and Preparative Chemistry & College of Chemistry,
Jilin University, Changchun 130012, China*

Available online 26 November 2007

Abstract

Fe-containing mesoporous materials (Fe-JLU-15) with various Si/Fe ratios (47–112) have been successfully synthesized by using semi-fluorinated surfactant of FSO-100 as a template. XRD, N_2 isotherm, and TEM techniques indicate that these samples have worm-like mesostructure with uniform pore size. UV–vis and ESR spectra suggest that Fe species in Fe-JLU-15 are mainly tetrahedrally coordinated. Interestingly, compared with Fe-SBA-15, the efficiency of incorporation of Fe species into Fe-JLU-15 is relatively high. Very importantly, catalytic data in benzylation of aromatic compounds such as benzene, toluene, and ethylbenzene with benzyl chloride shows that Fe-JLU-15 samples are very active and recycle catalysts.

© 2007 Elsevier B.V. All rights reserved.

Keywords: Fe-containing mesoporous materials; Fe-JLU-15; Benzylation; Semi-fluorinated surfactant

1. Introduction

Since a discovery of mesoporous silicas M41S [1] templated from surfactants, many potential applications have been used in the fields of catalysis [2], adsorption and separation [3], environmental monitoring [4], and fine chemicals [5]. However, pure silica materials could not be used in the particular application requirements, and thus special attention has been devoted to developing heteroatoms-containing mesostructured silica-based materials [2]. Among of them, Fe-containing MCM-41 has received much attention because of its unusual activity in alkylation and oxidation reactions [6–10]. Notably, Fe(III) ions trend to assemble hydroxide in alkaline media for the synthesis of MCM-41, which would block the pores, either partially or fully, thereby reducing the specific surface area, pore volume, and pore size [7]. Following the appearance of SBA-15 [11], many

researchers tried to introduce heteroatoms into SBA-15 using solely post-synthetic grafting [12] and immobilized [13] methods, mainly due to the difficulty of introducing heteroatoms in strongly acidic condition. Interestingly, Vinu et al. reported the direct synthesis Fe-SBA-15 by decreasing acidic strength of the solution [14], and the catalyst shows unusual reactive activity in Friedel–Crafts alkylations. However, it is a challenge to introduce Fe(III) ions in acidic solution into silica walls of SBA-15 with high efficiency. Recently, the synthesis of Fe-containing mesoporous materials has been extended to Fe-HMS [15] and Fe-FSM [16], and it is notable that Fe-HMS with crystalline ferric oxides shows lower activity in benzylation of benzene with benzyl chloride than Fe-SBA-15 [14].

More recently, a novel semi-fluorinated surfactant [FSO-100, $CF_3(CF_2)_4(EO)_{10}$] has been used to synthesize ordered mesoporous silica materials in both strongly acidic and neutral conditions [17]. Herein, we show highly efficient synthesis of Fe-containing mesoporous materials by using semi-fluorinated surfactant of FSO-100. Very importantly, these novel Fe-containing mesoporous materials exhibit

* Corresponding author. Fax: +86 431 85168624.

E-mail address: fsxiao@mail.jlu.edu.cn (F.-S. Xiao).

unusual catalytic activities in Friedel–Crafts alkylations, compared with conventional Fe-containing mesoporous materials such as Fe-SBA-15.

2. Experimental

2.1. Preparation of catalysts

In a typical synthesis of Fe-JLU-15, 0.8 g of FSO-100 was dissolved in 30 mL of H₂O, followed by addition of required amount of FeCl₃·6H₂O. The mixture was stirred at room temperature for 0.5 h. After addition of 1.25 mL of tetraethylorthosilicate (TEOS), the mixture was stirred at room temperature for 96 h. Then, the precipitate was transferred into an autoclave for further condensation at 100 °C for 48 h. The solid samples were collected by filtration and dried in air, followed by removal of surfactant template by acidified ethanol solution. Finally, the samples were calcined at 540 °C for 5 h, which are denoted as Fe-JLU-15(*x*), where *x* stands for the ratio of Si to Fe in the final product. For comparison, Fe-SBA-15 was prepared according the literature [14].

2.2. Catalyst characterization

Powder X-ray diffraction (XRD) data were recorded on a Siemens D5005 (45 kV, 40 mA) using nickel-filtered Cu K α radiation with wavelength of $\lambda = 1.5406$ Å. Transmission electron micrograph (TEM) was taken on a HITACHI H-8100 microscope operating at an accelerating voltage of 200 kV. Nitrogen adsorption isotherms were obtained at –196 °C on a Micromeritics TriStar. Samples were normally prepared for measurement by degassing at 200 °C under vacuum until a final pressure of 1×10^{-3} Torr was reached. Pore size distributions were calculated using the BJH method. The molar ratio of Si/Fe in samples was determined by the results of inductively coupled plasma analysis (ICP, Perkin-Elmer 3300DV). The diffuse reflectance UV–vis spectra for powder samples were obtained on a spectrometer Perkin-Elmer Lambda 20 UV–vis spectrometer equipped with an integrating sphere, and BaSO₄ was used as an internal standard. The electron spinning resonance (ESR) spectra were taken on a JEOL FA-200 spectrometer at room temperature. The signals were registered at microwave frequency of 9.4 GHz and microwave power of 0.998 mW with a sweep time of 240 s.

2.3. Catalytic tests

The liquid phase benzylation of benzene with benzyl chloride (BC) was carried out in a 50 mL three-necked round-bottomed flask equipped with a reflux condenser and heated in a precisely controlled oil bath under atmospheric pressure. In a typical run, 50 mg of catalyst, 6 mL of benzene, and 1 mmol of dodecane (internal standard) were added into the flask, followed by stirring for 30 min at required temperature (70 °C). Then, 0.5 mL of BC was finally added. The products were analyzed by gas chromatography (Varian CP-3800) with a FID detector.

3. Results and discussion

3.1. Characterization of Fe-JLU-15

Fig. 1 shows XRD patterns of Fe-JLU-15 with various Si/Fe ratios. Notably, all samples exhibit a broad peak in small-angle region, which indicates that these mesoporous materials were not well-ordered. Although FSO-100 template could be used to synthesize well-ordered mesoporous pure silica [16], the introduction of Fe species in this work reduces the ordering of mesostructure (Fig. 1), and similar phenomena have been reported previously [15,18,19]. Moreover, the *d* spacing of Fe-JLU-15 was slightly changed from 51 to 54 Å with the increase of Fe content (Table 1), which may be attributed that Fe–O bond is longer than Si–O bond. Additionally, it is difficult to find peaks in wide-angle region associated with crystalline iron oxides (Insert in Fig. 1), indicating the absence of bulky iron oxides in all samples.

Fig. 2 shows TEM image of Fe-JLU-15(86), giving worm-like mesostructure, which is in good agreement with one broad peak in XRD pattern (Fig. 1c).

Fig. 3 shows N₂ isotherms and pore size distributions of Fe-JLU-15 samples with various Si/Fe ratios, and their textural parameters are presented in Table 1. Notably, all samples exhibit typical IV-type curves, indicating their characteristic of mesostructure. Interestingly, pore size distributions of these samples are very uniform, giving at near 4.4 nm. However, the incorporation of Fe species into mesoporous materials has a significant effect on surface area and pore volume (Table 1), in agreement with heteroatoms substituted MCM-41 [20] and SBA-15 [14]. With changing Fe content from Si/Fe ratio of 112–47, the specific surface area and pore volume decreases from 1012 to 900 m² g^{–1}, and from 1.74 to 1.51 cm³ g^{–1}, respectively (Table 1).

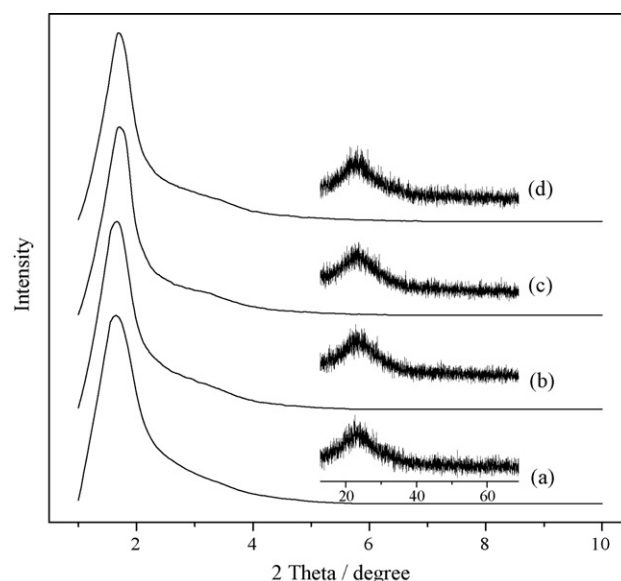


Fig. 1. Small-angle XRD patterns of Fe-JLU-15 with various Si/Fe ratios. (a) Fe-JLU-15(47), (b) Fe-JLU-15(70), (c) Fe-JLU-15(86), and (d) Fe-JLU-15(112). Insert is XRD patterns of corresponding samples in wide-angle region.

Table 1
Textural parameters of various samples^a

Samples ^b	Si/Fe		pH value of the initial gel	d (Å)	BET ($\text{m}^2 \text{g}^{-1}$)	d_p (nm)	V_p ($\text{cm}^3 \text{g}^{-1}$)
	Gel	Product ^c					
Fe-JLU-15(112)	30	112	2.5	51	1012	4.43	1.74
Fe-JLU-15(86)	25	86	2.4	52	1010	4.43	1.65
Fe-JLU-15(70)	20	70	2.4	54	936	4.44	1.61
Fe-JLU-15(47)	15	47	2.3	54	900	4.45	1.51
Fe-SBA-15(96) ^d	9	96	0.9	92	1024	9.3	1.35

^a Pore size distributions and pore volumes determined from N_2 adsorption isotherms at 77 K. d_p (pore diameter) and V_p (pore volume).

^b All samples were calcined at 540 °C for 5 h.

^c The Si/Fe ratios of samples were determined by ICP technique.

^d The data are from previous literature [14].

It is worth noting that the incorporation of Fe species into mesoporous silica walls in Fe-JLU-15 has much higher efficiency than that in Fe-SBA-15. As presented in Table 1, when Si/Fe ratio is 9.0 in initial gel, the final sample of Fe-SBA-15 exhibits Si/Fe ratio at 96. In contrast, when Si/Fe is 25 in initial gel, the final sample of Fe-JLU-15 exhibits Si/Fe ratio at 86. Possibly, the high efficiency of Fe species in JLU-15 is assigned to the unique synthetic conditions by using semi-fluorinated surfactant of FSO as a template. It has been shown that the synthesis of ordered mesoporous silica-based materials from semi-fluorinated surfactant has wide range of pH values (from strongly acidic to neutral conditions) [17]. In contrast, usual pH range for synthesis of SBA-15 from polymer surfactant (P123) is less than 2. Therefore, incorporation of iron species into mesoporous walls in Fe-JLU-15 samples under weak acidic conditions ($\text{pH} > 2$) is more efficient than that in Fe-SBA-15 samples strong acidic conditions ($\text{pH} < 2$).

Fig. 4 shows diffuse reflectance UV–vis spectra of Fe-JLU-15 with various Si/Fe ratios. All samples have displayed a broad band centered at 250 nm, which could be assigned to the

$d\pi\text{--}\pi\pi$ charge transfer between Fe and O atoms in the mesoporous walls of Fe–O–Si [21]. These results indicate that mostly Fe species still exist in the tetrahedral coordination environment, in agreement with previous reports [14,22,23]. However, there are additional bands between 350 and 550 nm

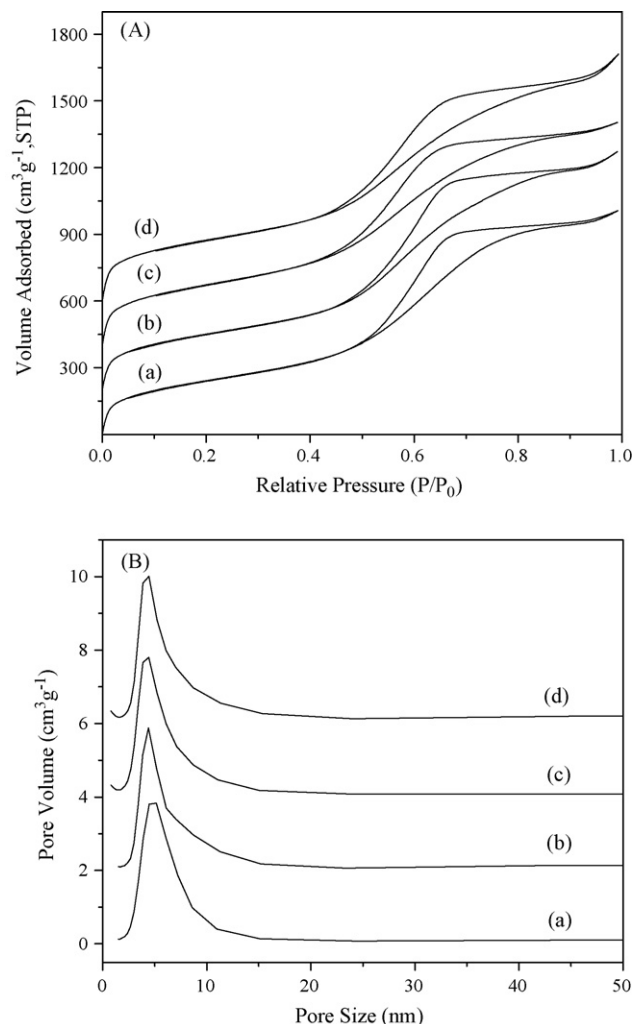


Fig. 3. N_2 adsorption isotherms (A) and pore size distribution (B) of Fe-JLU-15 with various Si/Fe ratios. (a) Fe-JLU-15(47), (b) Fe-JLU-15(70), (c) Fe-JLU-15(86), and (d) Fe-JLU-15(112). The isotherms (b), (c), and (d) removed upwards 200, 400, and 600 $\text{cm}^3 \text{g}^{-1}$ at the beginning for clarity, respectively.

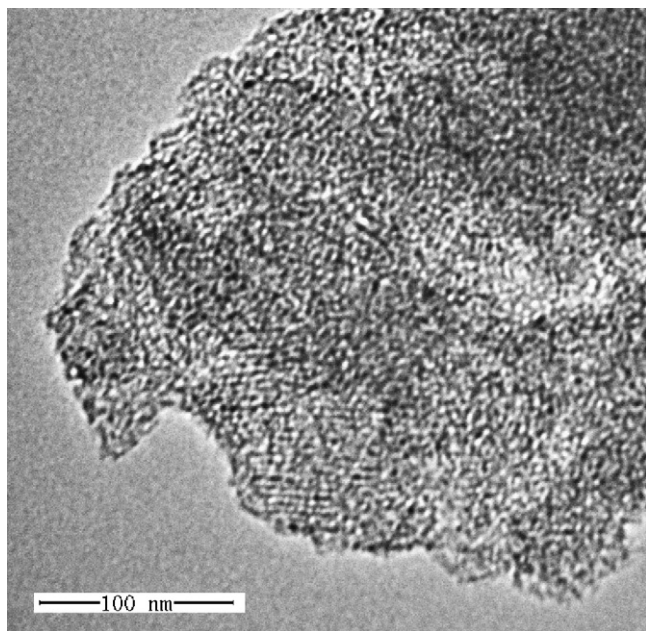


Fig. 2. TEM image of Fe-JLU-15(86).

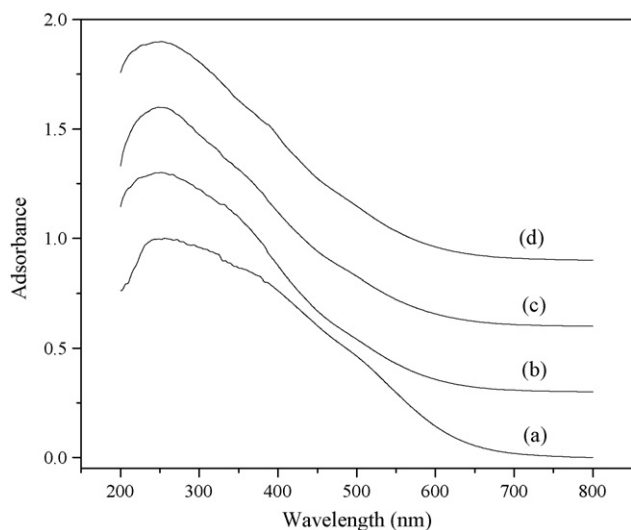


Fig. 4. UV-vis spectra of Fe-JLU-15 with various Si/Fe ratios. (a) Fe-JLU-15(47), (b) Fe-JLU-15(70), (c) Fe-JLU-15(86), and (d) Fe-JLU-15(112).

for Fe-JLU-15(47), indicating that there may be aggregative Fe species in this sample [24].

Fig. 5 shows ESR spectra of Fe-JLU-15 with various Si/Fe ratios. Notably, Fe-JLU-15(47) exhibits two signals at $g = 4.3$ and $g = 2.0$, and other samples exhibit one signal at $g = 2.0$. Generally, the signal at $g = 2.0$ could be assigned to tetrahedrally coordinated iron species (Fe^{3+}), while the signal at $g = 4.3$ is attributed to the clusters of iron oxides [25]. As observed in Fig. 5, the results indicate that Fe species in the Fe-JLU-15 is mainly tetrahedral coordination environment, which is quite coincident with the results by UV-vis spectra.

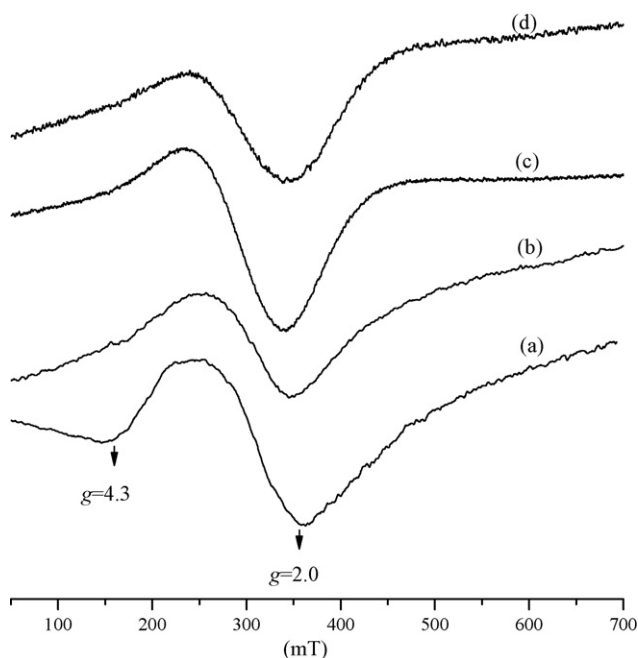


Fig. 5. ESR spectra of Fe-JLU-15 with various Si/Fe ratios. (a) Fe-JLU-15(47), (b) Fe-JLU-15(70), (c) Fe-JLU-15(86), and (d) Fe-JLU-15(112).

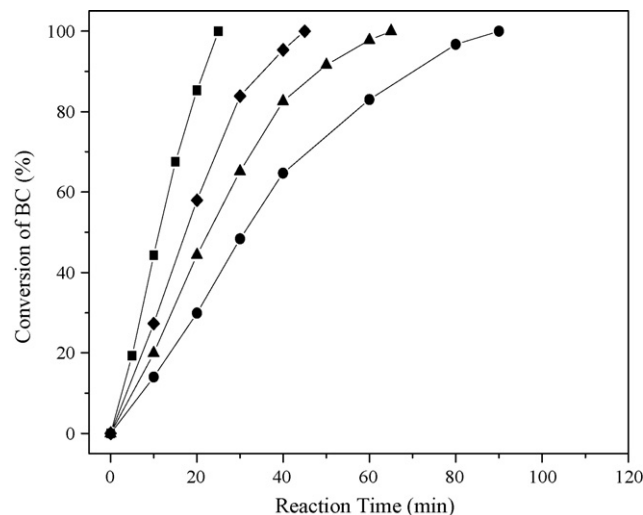


Fig. 6. Dependence of benzyl chloride conversion on reaction time over various catalysts at 70 °C. (■) Fe-JLU-15(47), (◆) Fe-JLU-15(70), (▲) Fe-JLU-15(86), and (●) Fe-JLU-15(112).

3.2. Friedel–Crafts alkylations

Friedel–Crafts alkylations constitute a very important class of reactions, which are of common use in organic chemistry. Among these reactions, the liquid-phase benzylation of benzene and other aromatic compounds such as benzyl chloride and benzyl alcohol is important for the production of diphenylmethane (DPM) and substituted diphenylmethanes, which are important industrially as intermediates for pharmaceuticals and fine chemicals [26]. Fe-containing mesoporous materials have been proved effective heterogeneous solid catalysts for benzylation of benzene in previous reports [7,14,15,27,28].

Fig. 6 shows the conversion of benzyl chloride (BC) in benzylation of benzene with benzyl chloride over Fe-JLU-15 catalysts with various Si/Fe ratios, and catalytic selectivity and turnover frequency (TOF) are presented in Table 2. The products in this reaction are diphenylmethane (DPM) and the isomers of dibenzylbenzene (DBB), 1,4-DBB, 1,3-DBB, and 1,2-DBB. Notably, all catalysts exhibit excellent catalytic activities, giving the complete conversion of BC in 25–90 min. Interestingly, the activities are strongly dependent on Fe loading in the samples. For example, it needs 90 min for near 100% conversion of BC over Fe-JLU-15(112) (run 1, Table 2), but it takes for 25 min over Fe-JLU-15(47) (run 5, Table 2).

Based on classical mechanism of Friedel–Crafts alkylations, one or more electron-donating groups in the aromatic ring will facilitate benzylation of an aromatic compound [26]. Unfortunately, as observed in Fe-SBA-15 [14] and Fe-HMS [15], catalytic activities are reduced by introduction of electron-donating groups in the aromatic compound, which are assigned to possible poisoning caused by the strong adsorption of the aromatic substrate [14]. Table 3 presents the conversion of BC and product selectivity in benzylation of aromatic compounds with various electron-donating groups such as methyl and methoxy over Fe-JLU-15(112) at 70 °C. For example, the

Table 2

Benzylation of benzene with benzyl chloride over various catalysts at 70 °C^a

Run	Catalyst	Time ^b (min)	Selectivity ^c (%)	TOF ^d (min ⁻¹)
1	Fe-JLU-15(112)	90	100	6.6
2	Fe-SBA-15(96)	70	100	7.2
3	Fe-JLU-15(86)	65	100	7.0
4	Fe-JLU-15(70)	45	98.5	8.2
5	Fe-JLU-15(47)	25	93.3	10

^a Reaction conditions: 6 mL of benzene, 0.5 mL of benzyl chloride, 50 mg of catalyst. The conversion was calculated from benzyl chloride.^b Time required for complete conversion of benzyl chloride.^c Selectivity for diphenylmethane.^d Moles of benzyl chloride converted per mole of Fe in the catalyst per min.

complete conversion of BC with benzene takes 120 min (run 1, Table 3), but the complete conversion of BC with toluene and anisole takes 25 (run 2) and 20 min (run 4, Table 3), respectively. These results indicate that electron-donating groups in the aromatic ring significantly facilitate benzylation over Fe-JLU-15(112) sample. It is also interesting to note that the time for complete conversion of BC with xylene (run 6) and ethylbenzene (run 7, Table 3) is longer than that of BC with toluene. Obviously, this case cannot be solely explained by the electron-donating groups because electron-donating ability in xylene and ethylbenzene is stronger than that in toluene. Possibly, in this case, steric effects may be another factor for the catalytic activity [29].

Additionally, when the conversion of BC reaches 100% in benzylation of toluene, the catalyst of Fe-JLU-15(112) was separated from the solution completely, followed by the addition of another 0.5 mL of BC. Interestingly, there is negligible BC conversion after reaction for 60 min, indicating that there is no leaching of catalytic sites (heterogeneous phenomenon) in Fe-JLU-15(112). Furthermore, after being

Table 3

Cenylation of substituted benzene with benzyl chloride over Fe-JLU-15(112) at 70 °C^a

Run	Aromatic compound	Time ^b (min)	Selectivity (%)	
			<i>o</i> -	<i>p</i> -
1	Benzene	120	–	100 ^c
2	Toluene	25	41.4 ^d	58.6 ^d
3	Toluene ^e	25	40.1 ^d	59.9 ^d
4	Anisole	20	34.1 ^f	65.9 ^f
5	Mesitylene	<10	100 ^g	–
6	<i>p</i> -Xylene	70	100 ^h	–
7	Ethylbenzene	50	34.3 ⁱ	65.7 ⁱ

^a Reaction conditions: 6 mL of benzene (or equivalent mole of substituted benzene), 0.5 mL of benzyl chloride, 30 mg catalyst. The conversion was calculated from benzyl chloride.^b Time required for complete conversion of benzyl chloride.^c Diphenylmethane.^d (*o*)-2-Methyl diphenylmethane, (*p*)-4-methyl diphenylmethane.^e The data were obtained after twice recycles.^f (*o*)-2-Methoxy diphenylmethane, (*p*)-4-methoxy diphenylmethane.^g 2,4,6-Trimethyl diphenylmethane.^h 2,5-Dimethyl diphenylmethane.ⁱ (*o*)-2-Ethyl diphenylmethane, (*p*)-4-ethyl diphenylmethane.

separated from the solution, the catalyst of Fe-JLU-15(112) was regenerated by calcination at 500 °C for 3 h. The regenerated catalyst still shows high activity in benzylation of toluene with BC, even if twice recycles Fe-JLU-15(112) still gives at near 100% BC conversion within 25 min (run 3, Table 3). Apparently, Fe-JLU-15 is an active and recycled catalyst for benzylation of aromatic compounds with BC.

4. Conclusion

In a summary, we have successfully synthesized Fe-containing mesoporous materials with high efficiency of Fe species into mesoporous walls from semi-fluorinated surfactant of FSO-100. Characterization of XRD and nitrogen isotherms indicates that Fe-JLU-15 samples are mesoporous ferrosilicates with high surface area and large pore volume. More importantly, Fe-JLU-15 samples as solid catalysts are very active for liquid-phase benzylation of aromatic compounds with BC.

Acknowledgements

The authors thank Prof. Keying Shi and Prof. Honggang Fu in Heilongjiang University at Harbin, China, for helpful discussion and support. This work was supported by the National Natural Science Foundation of China (20573044) and State Basic Research Project of China (2003CB615802).

References

- [1] C.T. Kresge, M.E. Leonowicz, W.J. Roth, J.C. Vartuli, J.S. Beck, *Nature* 359 (1992) 710.
- [2] A. Corma, *Chem. Rev.* 97 (1997) 2373.
- [3] H. Yang, A. Kuperman, N. Coombs, S. Mamicheafara, G.A. Ozin, *Nature* 379 (1996) 703.
- [4] R.M. Krishna, A.M. Prakash, L. Kevan, *J. Phys. Chem. B* 104 (2000) 1796.
- [5] W.F. Hoelderich, *Catal. Today* 62 (2000) 115.
- [6] N. He, S. Bao, Q. Xu, *Appl. Catal. A* 169 (1998) 29.
- [7] A. Corma, V. Fornés, M.T. Navarro, J. Pérez-Pariente, *J. Catal.* 148 (1994) 569.
- [8] A. Vinu, T. Krithiga, V. Murugesan, M. Hartmann, *Adv. Mater.* 16 (2004) 1817.
- [9] V. Parvulescu, B.-L. Su, *Catal. Today* 69 (2001) 315.
- [10] Q.H. Zhang, Q. Guo, X.X. Wang, T. Shishido, Y. Wang, *J. Catal.* 239 (2006) 105.
- [11] D. Zhao, J. Feng, Q. Huo, N. Melosh, G.H. Fredrickson, B.F. Chmelka, G.D. Stucky, *Science* 279 (1998) 548.
- [12] Z. Luan, M. Hartmann, D. Zhao, W. Zhou, L. Kevan, *Chem. Mater.* 11 (1999) 1621.
- [13] X.S. Zhao, G.Q. Lu, C. Song, *Chem. Commun.* (2001) 2306.
- [14] A. Vinu, D.P. Sawant, K. Ariga, K.Z. Hossain, S.B. Halligudi, M. Hartmann, M. Nomura, *Chem. Mater.* 17 (2005) 5339.
- [15] K. Bachari, J.M.M. Millet, B. Benaïchouba, O. Cherifi, F. Figueras, *J. Catal.* 221 (2004) 55.
- [16] M.M. Mohamed, N.A. Eissa, *Mater. Res. Bull.* 38 (2003) 1993.
- [17] X. Meng, Y. Di, L. Zhao, D. Jiang, S. Li, F.-S. Xiao, *Chem. Mater.* 16 (2004) 5518.
- [18] H. Matsushashi, M. Tanaka, H. Nakamura, K. Arata, *Appl. Catal. A* 208 (2001) 1.
- [19] M.S. Ghattas, *Micropor. Mesopor. Mater.* 97 (2006) 107.
- [20] M. Kruk, M. Jaroniec, A. Sayari, *Langmuir* 15 (1999) 5683.

- [21] B. Echchahed, A. Moen, D. Nicholson, L. Bonneviot, *Chem. Mater.* 9 (1997) 1716.
- [22] Y. Wang, Q. Zhang, T. Shishido, K. Takehira, *J. Catal.* 209 (2002) 186.
- [23] Y. Han, X. Meng, H. Guan, Y. Yu, L. Zhao, X. Xu, X. Yang, S. Wu, N. Li, F.-S. Xiao, *Micropor. Mesopor. Mater.* 57 (2003) 191.
- [24] Y. Sun, S. Walspurger, J.-P. Tessonnier, B. Louis, J. Sommer, *Appl. Catal. A* 300 (2006) 1.
- [25] D. Goldfarb, M. Bernardo, K.G. Strohmaier, D.E.W. Vaughan, H. Thormann, *J. Am. Chem. Soc.* 116 (1994) 6344.
- [26] G.A. Olah, *Friedel–Crafts Chemistry*, Wiley, New York, 1973.
- [27] V.R. Choudhary, S.K. Jana, B.P. Kiran, *Catal. Lett.* 59 (1999) 217.
- [28] V.R. Choudhary, S.K. Jana, *Appl. Catal. A* 224 (2002) 51.
- [29] M.S. Newman, *Steric Effects in Organic Chemistry*, John Wiley & Sons, Inc., New York, 1956.